

Improved pH reliability of solution-processed In_2O_3 field-effect transistors via Ga doping and different annealing temperatures

¹JoonHui Park, ²Jeongsoo Hong, ²Kyung Hwan Kim, ¹You Seung Rim*

¹School of Intelligent Mechatronics Engineering, Sejong University, Seoul 05006, Republic of Korea

²Department of Electrical Engineering, Gachon University, Seongnam 13120, Republic of Korea

*E-mail: youseung@Sejong.ac.kr

Keywords: Oxide semiconductor, solution process, biosensor, electrolyte gated transistor

ABSTRACT

Studies of metal oxide semiconductors-based biosensors have focused on detection properties done typically by specific target receptor attachment. However, the exploration of metal oxide semiconductors with different physical and chemical properties has still not been considered widely through an understanding of the liquid-solid interface. In this study, we examined the effect of different Ga content on solution-processed indium oxide films and their transistors. As a result, we confirmed that surface defects could be suppressed by the addition of Ga, which affected the pH reliability of devices under different pH environments.

focused on the feasibility and realization of specific target monitoring (i.e., blood glucose, pH, virus, DNA, etc.) [9].

Here, we report the effect of several fabrication conditions and Ga doping on solution-processed indium oxide (In_2O_3) TFTs to explore the dependency of oxygen vacancies and crystal structures for a pH sensor. We confirmed that the magnitude of oxygen vacancies impacts instability in various pH conditions and could be suppressed effectively by Ga doping and increased annealing temperatures.

In our results, we found that the precise control of the surface passivation of metal oxide semiconductors was an important factor for realizing electrolyte-gated transistors with the exposed surface of metal oxides.

1 INTRODUCTION

Oxide semiconductors have been studied in display backplane technologies due to their high reliability, mobility, and the permissibility of the amorphous structure for high electrical uniformity [1,2]. Many material candidates have been considered, such as indium-based or indium-free ternary or quaternary systems (i.e., IGZO, ITZO, ITGO, ZTO, AZTO, HIZO, etc.) [3]. Based on these efforts, IGZO-based thin-film transistors (TFTs) have been commercialized and many researchers are now searching for new era applications of metal oxide TFTs [4].

Recently, electrical sensor platforms have attracted increased attention in the fields of biosensors, healthcare monitoring, touch sensors, and photonic sensors [5, 6]. Among them, TFT-based metal oxide biosensors are highly fascinating for non-invasive body fluid monitoring applications due to high sensitivity and selectivity. Specifically, diabetes monitoring with TFT-based biosensors have been realized by sputtered/solution-processed metal oxide TFTs [7].

Intrinsic metal oxide semiconductors have oxygen vacancies, and this contributes to an increase in carrier concentrations and deterioration of reliability under electrical stress and/or illumination [2]. In comparison, metal oxide TFT-based biosensors can operate in a liquid and the above issues can be addressed in a number of ways [8]. Thus, it is essential to consider the complexity of the liquid/solid interface under device operation. Most previous biosensor research with oxide TFTs have

2 EXPERIMENT

2.1 Synthesis of organic and aqueous solution-based metal precursor solutions

Indium oxide precursor solutions with varying ligands were synthesized by dissolving 0.1M of indium nitrate hydrate ($\text{In}(\text{NO}_3)_3 \cdot x\text{H}_2\text{O}$, Aldrich, 99.999%) in 2-methoxyethanol ($\text{C}_3\text{H}_8\text{O}_2$, Aldrich, 99%) and water (H_2O , Aldrich). For the Ga doping, gallium nitrate hydrate ($\text{Ga}(\text{NO}_3)_3 \cdot x\text{H}_2\text{O}$, Aldrich, 99.999%) was added in indium oxide precursors (In:Ga molar ratio = 10 : 0.1). After stirring vigorously for 10 h at room temperature, the solutions appeared transparent and homogeneous.

2.2 Device fabrication

p^{++} boron-doped Si wafers with thermally grown SiO_2 (100 nm) were sequentially cleaned in acetone and isopropyl alcohol and then treated by oxygen plasma treatment for 5 min. The In_2O_3 or Ga doped In_2O_3 (GIO) precursor solutions were spin-coated on substrates at 3000 rpm for 30 s. The samples were then soft-baked at 100 °C for 10 min and then annealed at varying temperatures (250–550°C) for 3 h. Ga doped In_2O_3 conditions were annealed at 350°C for 3 h. The Ti (20 nm)/Au (40 nm) source and drain (S/D) electrodes were deposited sequentially by E-beam evaporation with a metal shadow mask. The channel region was defined by a width (W) of 1000 μm and a length (L) of 200 μm .

The substrate was incubated in a 1 mM ethanolic

solution of 1-dodecanethiol (DCSH) for passivation of the Au surface for 1 h. After thorough rinsing with ethanol, a 1 mM ethanolic solution of (3-aminopropyl)trimethoxysilane (APTES) was incubated as the passivation of the metal oxide surface for 1 h, and the substrate was immersed in etOH.

2.3 Material and device characterization

The chemical and structural properties of In_2O_3 and GaO oxide films were examined using X-ray photoelectron spectroscopy (XPS) and X-ray diffractometer (XRD), respectively. The TFT characteristics of the devices were measured in ambient air using a Keithley SCS-4200 semiconductor parameter analyzer. We prepared pH buffer solutions with a range of 2 – 10 for electrolyte gating. Polydimethylsiloxane (PDMS) pools were used to confine the solution and a reference electrode (Ag/AgCl) was put in the pool as the gate electrode.

3 RESULTS

3.1 Effect of annealing temperatures

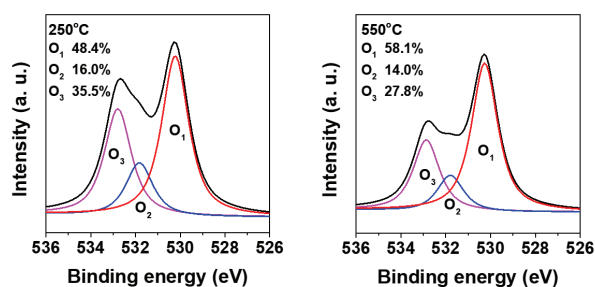


Fig. 1 O1s XPS results of 250 and 550°C In_2O_3 films

Fig. 1 shows the O1s XPS results of In_2O_3 films for different annealing temperatures. Three different Gaussian peaks assigned in the metal-oxide lattices (O_1), the oxygen deficient state (O_2), and the chemisorbed or dissociated oxygen states or OH^- impurities (O_3) [10]. With an increase in annealing temperature from 250 to 550°C, O_2 and O_3 peaks were significantly decreased due to the dihydroxylation of metal hydroxide films and the formation of more stoichiometry compositions close to the In_2O_3 .

Fig. 2 shows AFM images and RMS values of In_2O_3 films for the different annealing temperatures. The RMS value for 550°C In_2O_3 was higher than that of 250°C In_2O_3 films. This could be attributed to improved crystallinity, which was confirmed by the XRD results. Grain size at 250°C and 550°C were 7.5 nm and 9.4 nm, respectively.

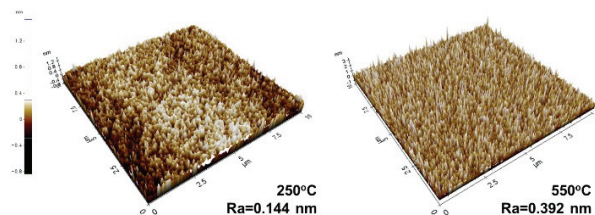


Fig. 2 AFM images and RMS values of 250 and 550°C In_2O_3 films

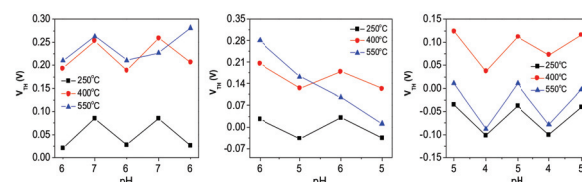


Fig. 3 pH hysteresis of In_2O_3 for the different annealing temperatures under the range of 4 to 7.

Fig. 3 shows pH hysteresis of In_2O_3 based EGTs for the different annealing temperatures. The pH value changed as follows: (6 → 7 → 6), (6 → 5 → 6), (5 → 4 → 5). Threshold voltage (V_{TH}) values were extracted at each pH. With an increase of annealing temperature, V_{TH} variations gradually increased. Typically, the oxygen deficiency of metal oxide semiconductors results in the instability of devices. Thus, it was expected that less-oxygen deficient In_2O_3 films would have better performance in device operation. However, the results showed the opposite behavior with a decrease of oxygen deficiency. This result is quite questionable, but we think that degenerative In_2O_3 with high temperature annealing films could be affected by proton penetration as the donor site, which could increase carrier concentration that is recovered slowly [11]. Also, grain boundary scattering (regarding trap sites) and proton intercalation can affect variations of hysteresis for the different annealing temperatures of In_2O_3 films. Therefore, 250°C In_2O_3 EGTs showed the best performance.

3.2 Effect of Ga doping on In_2O_3

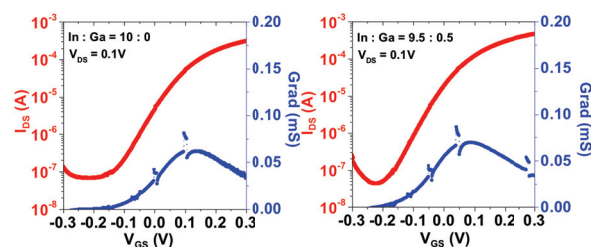


Fig. 4 Transfer curves and transconductance of In_2O_3 and Ga doped In_2O_3 EGTs.

Ga doped In_2O_3 -based EGTs were more stable and had a higher on/off ratio, and maximum transconductance (gm_{max}) compared to undoped In_2O_3 .

These could be attributed to the reduction of oxygen deficiency on the surface of In_2O_3 due to Ga doping. We confirmed that the O_2 area of $\text{O}1\text{s}$ peaks were reduced when Ga was doped in In_2O_3 , which is shown in Fig. 5. We also tested V_{TH} variations of In_2O_3 and Ga doped In_2O_3 EGTs under continuous pH changes as shown in Fig. 6. Hysteresis is a critical issue to realize continuous pH or for disease monitoring sensors. Thus, devices were tested under different pH steps with both increments (3 to 5 and 7 to 9) and decrements (5 to 3 and 9 to 7), separately.

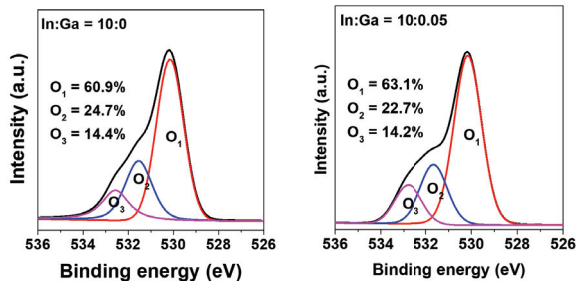
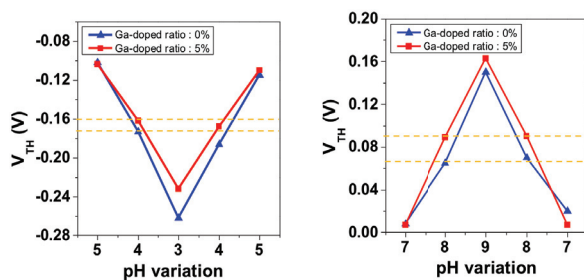


Fig. 5 $\text{O}1\text{s}$ XPS results of In_2O_3 and Ga doped In_2O_3 films

With a decrease of pH (5 to 3), undoped In_2O_3 EGTs showed higher sensitivities than that of Ga doped In_2O_3 . Meanwhile, V_{TH} values of undoped In_2O_3 did not show bigger different values than those of Ga doped In_2O_3 when the pH was increased from 3 to 5. Within the pH ranges of 7 – 9 and 9 – 7, Ga doped In_2O_3 had higher sensitivity and less hysteresis than that of undoped In_2O_3 . This could be attributed to the reduction of oxygen deficiency and the suppression of proton penetration through oxygen deficient sites.



4 CONCLUSIONS

We examined the effect of different post-annealing temperatures and gallium doping concentrations on solution-processed In_2O_3 -based EGTs. Morphologies and oxygen deficiency depended on annealing temperature and Ga content. With variations in pH values, non-doped In_2O_3 EGTs were unstable and did not recover to previous values due to the trapped electrons resulting from oxygen deficiency. For annealing temperatures, higher temperature annealed devices had unstable behavior. This could be attributed to the grain boundary effect or

degenerative semiconductor behavior with proton penetration.

REFERENCES

- [1] J. S. Park, W.-J. Maeng, H.-S. Kim, J.-S. Park, "Review of recent developments in amorphous oxide semiconductor thin-film transistor devices," *Thin Solid Films*, Vol. 520, No. 6, pp. 1679-1693 (2012).
- [2] K. Ide, K. Nomura, H. Hosono, "Electronic defects in amorphous oxide semiconductors: a review," *Phys. Stat. Solidi A*, Vol. 216, No. 5, pp. 1800372 (2019).
- [3] E Fortunato, P Barquinha, R Martins, "Oxide semiconductor thin - film transistors: a review of recent advances," *Adv. Mater.* Vol. 24, No. 22, pp. 2945-2986 (2012).
- [4] John F. Wager, "Oxide TFTs: A progress report," *Inf. Disp.* Vol. 32, No. 1, pp. 16-21 (2016).
- [5] D Wang, V Noël, B Piro, "Electrolytic gated organic field-effect transistors for application in biosensors—a review," *Electronics*, Vol. 5, No. 1, pp. 9 (2016).
- [6] S. Lee, S. Jeon, R. Chaji, A. Nathan, "Transparent semiconducting oxide technology for touch free interactive flexible displays," *Proc. IEEE*, Vol 103, No. 4, pp. 644-664 (2015).
- [7] J. W. Park, B. H. Kang, H. J. Kim, "A review of low - temperature solution - processed metal oxide thin - film transistors for flexible electronics," *Adv. Func. Mater.* DOI:10.1002/adfm.201904632.
- [8] J Y. S. Rim, S.-H. Bae, H. Chen, J. L. Yang, J. Kim, A. M. Andrews, P. S. Weiss, Y. Yang, H.-R. Tseng, "Printable Ultrathin Metal Oxide Semiconductor-Based Conformal Biosensors," *ACS Nano* Vol. 9, No. 12, pp. 12174-12181 (2015).
- [9] Y. S. Rim, H. Chen, B. Zhu, S. H. Bae, S. Zhu, P. J. Li, I. C. Wang, Y. Yang, "Interface engineering of metal oxide semiconductors for biosensing applications," *Adv. Mater. Interfaces* Vol. 4, No. 10, pp. 1700020 (2017).
- [10] A. Gurlo, M. Ivanovskaya, A. Pfau, U. Weimar, W. Göpel, "Sol-gel prepared In_2O_3 thin films," *Thin Solid Films*, Vol. 307, No. 1-2, pp. 288-293 (1997).
- [11] Pedro Estrela, "Introduction to biosensors," *Essays. Biochem.* Vol 60, No. 1, pp. 1-8 (2016).